JOURNAL OF FORENSIC SCIENCES

J Forensic Sci, January 2012, Vol. 57, No. 1
doi: 10.1111/j.1556-4029.2011.01920.x
Available online at: onlinelibrary.wiley.com

PAPER

ANTHROPOLOGY

Richard A. Gonzalez,[1,2] *Ph.D.*

Determination of Sex from Juvenile Crania by Means of Discriminant Function Analysis*,†

ABSTRACT: This study provides evidence of craniofacial growth variation between the sexes in juveniles of European descent. Data were collected from lateral cephalometric radiographs belonging to the Michigan Craniofacial Growth Study. The collection consists of longitudinal lateral radiographs that represent individuals 5–16 years of age. Each radiograph was manually traced on hyprint vellum from which eight craniometric points were identified. From these points, 20 craniofacial measurements were recorded and then analyzed by means of a canonical discriminant function analysis. Sex classification equations were then created by applying a backward stepwise procedure to the discriminant functions. The analysis demonstrates the presence of sexually dimorphic differences in craniofacial growth. The neurocranium is the most sexually dimorphic region of the juvenile craniofacial skeleton, until the onset of puberty. Size is the main source of variation with males having taller and longer heads than females. Overall, sex classification in the sample ranges from 78 to 89% accuracy.

KEYWORDS: forensic science, forensic anthropology, sexual dimorphism, sex determination, craniofacial growth, skull identification

Two thousand four hundred and eighty-seven juveniles between the ages of 5 and 16 were homicide victims in the United States from 2004 to 2007. Most juvenile homicides were committed against males, the majority of which occurred between the ages of 13–16 (1–4). The trends in juvenile victimization coupled with the fact that many juvenile skeletal remains are recovered in archaeological settings, make the development of forensic anthropological techniques for juvenile skeletal identification a necessity. There are numerous identification issues in the archaeological and forensic analysis of juvenile skeletons; sex determination is the most important because sex is not as easily identifiable in juveniles as it is in adults.

Determination of sex is a vital aspect of skeletal analysis and the key for establishing skeletal profiles of unidentified individuals (5,6). Previous studies have attempted to develop sex identification standards for juvenile skeletal material, and a large body of work has accumulated concerning morphological differences that center on those regions that are most sexually dimorphic in adults, the skull, and pelvic girdle (7–24). Unfortunately, many of these attempts to develop sex identification standards for juvenile skeletal remains have provided variable degrees of accuracy and according to Komar and Buikstra (25), "have failed to find convincing evidence of sexual dimorphism in preadolescent skeletons" (p. 126). Consequently, the determination of sex remains the single biggest problem in the analysis of juvenile skeletal remains (26,27).

The advent DNA technology and its application in archaeological and forensic investigations (28,29) facilitated the development of new techniques for analyzing skeletal material (27). Sex typing of genetic material made possible the identification of sex differences in juvenile skeletal remains (30). In particular, the amelogenin gene, which is present on both the X and Y chromosomes, is very useful for sex identification (31–34). Researchers have also attempted to extract and amplify samples of nuclear and mitochondrial DNA from skeletal remains utilizing PCR and short tandem repeat (STR) technology with a good level of success (35–39).

Despite the promise of genetic profiling in forensic and archaeological investigations, there are limitations with DNA extraction from bone because of consistent problems relating to contamination, degradation, timing, and expense (40–44). Additionally, Yao et al. (45) identified base shifts, reference bias, phantom mutations, base miscoding, and artificial recombination as sources of error during the forensic analysis of genetic material (45).

Moreover, long-term exposure to natural forces greatly affects the integrity of skeletal remains. In such cases, only minute amounts of genetic material survive in bone, making extraction and contamination the biggest problem in the genetic analysis of skeletal remains (43). DNA reproducibility is severely affected during PCR or STR analysis. Inhibitors, such as fulvic acids, that are inherent or introduced to bone by the environment further complicate DNA analysis (46–48). For example, research by Gilbert et al. (49,50) demonstrated that damage to DNA can result in changes in the sequences mimicking other DNA sequences. A damaged sample of European mtDNA may resemble a Near Eastern mtDNA sequence (43).

Even though genetic profiling holds great promise in the sex identification of juvenile remains, the concerns mentioned previously require the development of methodologies that focus on the

[1]Department of Anthropology, St. Lawrence University, 23 Romoda Drive, Canton, NY 13617.
[2]Current address: Department of Physical Therapy, Clarkson University, Clarkson Hall, 59 Main St., Potsdam, NY 13699.

*Presented in part at the 76th Annual Meeting of the American Association of Physical Anthropologists, March 28–31, 2007, in Philadelphia, PA, and at the 60th Annual Meeting of the American Academy of Forensic Sciences, February 18–23, 2008, in Washington DC.
†Partially funded by the St. Lawrence University Jeffrey Campbell Graduate Fellowship.
Received 24 June 2010; and in revised form 1 Nov. 2010; accepted 27 Nov. 2010.

quantitative and morphological analysis of juvenile skeletons. In the event that DNA identification is available, quantitative and morphological analyses of juvenile remains can corroborate the results. However, if DNA identification is not possible, then quantitative and morphological assessments serve as the only sources of identification.

This study contributes to the literature concerning sex determination in juvenile skeletal remains by identifying sex-specific patterns of craniofacial growth and development. The craniofacial skeleton is the best source for sex identification in juveniles because it reaches maturity early in life (51–53). Neurocranial growth tends to slow down from about 2.5 years of age with much of craniofacial morphology already established by the time the first permanent molar has erupted (51–53). As a result, sex-specific features should be present early in craniofacial development.

Previous studies by Ceballos and Rentschler (54), Townsend et al. (55), Hsiao et al. (56), Patil and Mody (57) and Veyre-Goulet et al. (58) have relied on cephalometric radiographs to develop discriminant functions for craniofacial sex identification. Unfortunately, their work has only involved the study of adults. Aside from the present investigation, Bulygina et al. (59) published a study on the ontogeny of facial sexual dimorphism in which they suggest that craniofacial sex differences establish early in development and that such difference vary according to age. However, their work only focuses on the face.

This study provides further insights into the development of craniofacial sexual dimorphism. By analyzing metric data collected from cephalometric radiographs, this study aims to identify possible craniofacial growth differences between males and females and provide a set of discriminant function equations that may aid in the identification of sexual dimorphism in juvenile skeletal remains.

Materials and Methods

Data Collection

This study relies on metric data collected from lateral cephalometric radiographs housed at the Department of Orthodontics, University of Michigan-School of Dentistry, to identify sexually dimorphic differences in craniofacial growth (60). The Michigan Craniofacial Growth Study collection is one of the most extensive and best-documented sources of craniofacial growth data in the United States (60–62). The original sample consists of a longitudinal growth series of 83 individuals (47 males and 36 females) of European descent. These films represent an average local school population from the Ann Arbor, Michigan area (60,62). All radiographs were standardized and taken on the subject's birthday or 6 months thereafter from the ages of 5–16 (60,62).

To conduct the present study, 25 males and 25 females were randomly selected for each specific year. As variation in growth prevents the identification of calendar age, the sample was organized into age-groups modeled after the pattern of dental eruption. The sample was randomly re-selected for each age-group to analyze the data cross-sectionally. Treating the data cross-sectionally leads to more conservative results (63). Hence, it is unlikely that this study will show sex differences in craniofacial growth that do not exist. Therefore, the original longitudinal sample of 83 individuals was converted into a cross-sectional sample of 598 individuals of European descent with a range of 5–16 years of age (Table 1). The 5–16 age range corresponds to the earliest stage at which brain/cranial growth nears completion and the period preceding adulthood. Also, analyzing the data chronologically presents an opportunity to observe how sex-specific differences develop on a year-by-year basis.

Metric data were collected by manually tracing 11 × 14 lateral cephalometric radiographs using a 0.05-mm mechanical pencil. All data were collected by means of cephalometric tracing because manual tracing of films provides a physical representation of the data. Even though it is more time-consuming and old-fashioned, the study chose manual tracing of cephalograms for data collection because it provides a physical representation of the data, which enables an appreciation of morphological changes throughout development. Each radiograph was traced onto 11 × 17-hyprint vellum on top of a portable light box. After tracing the radiographs, eight craniometric points (Fig. 1) were identified and marked film-by-film. From these points, the study recorded 20 measurements in millimeters using a Mitutoyo Mycal E-Z 300 mm digital sliding caliper (Mitutoyo America Corporation, Aurora, IL) (Table 2).

Data Analysis

This investigation used The Statistical Package for the Social Sciences (SPSS) version 17.0 for data input and analysis (67). All raw data were converted to natural size using the calibration scale provided by Dibbets and Nolte (68). According to Dibbets (62), the data of the Michigan Craniofacial Growth Study (60) were

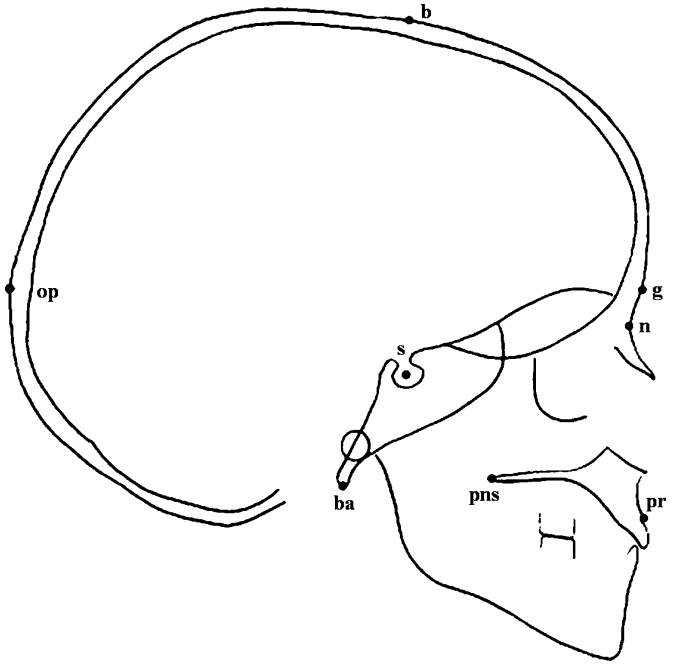

FIG. 1—*Cephalometric tracing with craniometric points. Points are defined as: basion (ba); bregma (b); glabella (g); nasion (n); opisthocranion (op); posterior nasal spine (pns); prosthion (pr); and sella (s). Figure from Gonzalez (61).*

TABLE 1—*Selected sample for the study.*

Age-Group	Females	Males	Total
5–6	50	50	100
7–8	50	50	100
9–11	50	50	100
11–12	50	50	100
13–14	50	50	100
15–16*	49	49	98

*Two tracings had to be discarded from the analysis.

collected by using a Whemer headholder (The WEHMER Corporation, Lombard, IL) to keep the head still when taking the cephalogram. This method accepts a distance of 60 inches for the focal-to-midsagittal plane and a distance of 7.75 inches for the midsagittal-to-film distance. To calculate the percentage enlargement, the focal-to-midsagittal plane distance is added to the midsagittal-to-film distance and then divided by the focal-to-midsagittal plane distance. Thus, $(60 + 7.75)/60 = 1.129$, which means that the films have an enlargement factor of 12.9%. To calibrate the data, one must divide 1 by 1.129, which yields a ratio of 0.886. All the measurements collected from a cephalogram must then be multiplied by 0.886 to convert to natural size (62). Dibbets (62) and Dibbets and Nolte (68) tested the reliability of the size correction equation and determined that the corrections for enlargement removed the magnification bias from the data. Thus, the size-adjusted data shows clear-cut morphological variation in the sample (62,68).

Once all data were calibrated, the sample was organized according to sex and age-group to facilitate statistical analysis. Discriminant functions by way of canonical correlations provided the necessary insight into possible sex differences in the sample. In this study, a canonical correlation discriminant function analysis for all age-groups aided in the identification of sex-specific differences throughout development (69). Canonical discriminant analyses allow the study of between-group variation by analyzing multiple variables simultaneously (70). A series of linear combinations of the variables produce a series of functions with a set of coefficients. Each function is independent of the other so that the group means between the functions are as different as possible (70). Consequently, each of the canonical discriminant functions represents one aspect that contributes to group variation (71). The first few functions are sufficient to explain all the important factors relating to the variation expressed by the data. These functions serve to create statistical associations between the discriminant scores and the groups in the analysis and then allocate each group to a proper membership (67,72,73). The values of these functions, which were plotted in a multidimensional space, provide a graphical representation of each canonical function and insight regarding sex variation within each age-group (74).

Sex classification equations were then created by applying a backward stepwise procedure to the discriminant functions. Those variables that contributed the least to sex identification were eliminated from the analysis. Thus, the equations rely on the variables that are most statistically associated with sex. The average of the function centroids, within each discriminant formula, created sectioning points between males and females. Each classification model was then cross-validated by using the leave-one-out function of the canonical discriminant function analysis procedure.

TABLE 2—*Variables used in the analysis.*

Code	Name
GOL	Glabella–Opisthocranion
NOL	Nasion–Opisthocranion
NBL	Nasion–Bregma
BOL	Bregma–Opisthocranion
OBL	Opisthocranion–Basion
BBL	Basion–Bregma
BPL	Basion–Prosthion
BNL	Basion–Nasion
BSL	Basion–Sella
NSL	Nasion–Sella
NPL	Nasion–Prosthion
PBL	PNS–Basion
PPL	PNS–Prosthion
PNL	PNS–Nasion
SPL	Sella–PNS
PSL	Prosthion–Sella
SGL	Sella–Glabella
SOL	Sella–Opisthocranion
OPL	Opisthocranion–Prosthion
PBR	Prosthion–Bregma

Based on definitions provided by Bass (64), Enlow (65), and Howells (66).

Results

Three of the 20 functions produced by the canonical discriminant function analysis were the most statistically significant and account for 87.3% of the total variation (Table 3). Results from each of these canonical discriminant functions represent metric differences in craniofacial form between the sexes throughout development. The first canonical discriminant function (CAN1) accounts for 71.9% of the total variance (Table 4) and displays high loadings for PNS–nasion length (PNL), PNS–prosthion length (PPL), nasion–prosthion length (NPL), prosthion–sella length (PSL), and basion–nasion length (BNL). The pattern of variation in this axis represents important developmental changes in the craniofacial skeleton as it grows over time (Fig. 2). A combination of facial and neurocranial variables are most significant in this axis. CAN1 illustrates sequences of developmental differences between the sexes in the facial skeleton and that an interaction with neurocranial growth determines the growth trajectory of the face. Both sexes show a similar developmental transition from childhood to puberty. This transition occurs at the 11–12 age-group when there is a trend toward greater facial development. However, there are periods in which facial size increase is slow, and there are periods in which facial size increase is faster.

The position of the age-groups 5–6 and 11–12 in CAN1 suggests slow or decreased facial changes throughout development in these two age-groups. Male and female differences at these two age-groups are only slightly evident. For the other age-groups, size tends to change exponentially and as these facial size changes occur, so does sexual dimorphism. In the earlier age-groups, female facial growth is much faster and, consequently, females appear much larger than males. At the transition into puberty, female facial growth decreases and male facial growth increases. Therefore, males appear much larger than females. The ages 5–6 and 11–12 represent a reduction of craniofacial growth.

The second canonical discriminant function (CAN2), which accounts for 10.6% of the total variance (Table 4), displays high loadings for sella–glabella length (SGL), PNS–prosthion length (PPL), bregma–opisthocranion length (BOL), nasion–prosthion length (NPL), and prosthion–sella length (PSL). The pattern of variation in this axis represents an illustration of craniofacial developmental growth velocity curves between the sexes (Fig. 3). Both sexes follow a similar pattern of growth velocity in which there are increases and decreases in the rate of craniofacial growth. A developmental transition from childhood to puberty is also evident at the 11–12 age-groups. At this point in development, both sexes go from a slowdown of craniofacial development, to having a slight increase in craniofacial growth during puberty. CAN2 clearly illustrates that the majority of craniofacial growth is completed around the age of six. The slight increases at the onset of puberty reflect the development of secondary sexual characteristics.

In the third canonical discriminant function (CAN3), which accounts for 4.8% of the total variance (Table 4), high loadings are displayed for basion–bregma length (BBL), nasion–bregma length (NBL), sella–glabella length (SGL), bregma–opisthocranion length (BOL), and glabella–opisthocranion length (GOL). The pattern of

TABLE 3—*Summary of canonical discriminant functions.*

Function	Wilks' Lambda	Eigenvalue	% Variance	Cumulative %	Canonical Correlation	$p > 0.05$
CAN1	0.030	5.059	71.9	71.9	0.914	0.000
CAN2	0.182	0.746	10.6	82.5	0.654	0.000
CAN3	0.319	0.335	4.8	87.3	0.501	0.000

TABLE 4——*Structure matrix.*

Variable	CAN1	CAN2	CAN3
PNL	0.766*	−0.275	0.097
PPL	0.687*	0.044*	−0.198
NPL	0.676*	−0.018*	0.026
PSL	0.654*	−0.067*	0.070
BNL	0.624*	−0.245	0.340
PBR	0.576	−0.100	0.389
BPL	0.522	−0.101	0.038
BSL	0.521	−0.329	0.225
SPL	0.462	−0.295	0.180
NSL	0.452	−0.120	0.399
BBL	0.368	−0.227	0.715*
NBL	0.287	−0.147	0.526*
SGL	0.452	0.139*	0.511*
BOL	0.212	−0.005*	0.464*
GOL	0.368	−0.080	0.462*
NOL	0.383	−0.142	0.411
OPL	0.412	−0.127	0.206
OBL	0.043	−0.131	0.213
PBL	0.167	−0.127	0.244
SOL	0.166	−0.104	0.235

*Largest absolute correlation between each variable and any discriminant function.

variation in this axis expresses sex differences within the sample (Fig. 4). Neurocranial variables illustrate most of the variation in this function. These variables represent clear-cut differences between the sexes, which develop early in life. As craniofacial growth nears completion around the age of six, it is expected that neurocranial morphology in females and males would already be established by this period. Further development of secondary sexual characteristics is the result of enhancements of already established craniofacial features that are unique to males and females.

Figure 5 is a two-dimensional plot of the first and second canonical discriminant functions, which collectively account for 82.5% of the total variance. This plot illustrates facial growth changes throughout development (CAN1) and the developmental trajectories between the sexes because of differences in craniofacial growth velocity (CAN2). In comparing these two canonical axes, one can observe a separation of the sample according to sex and age-group category. The sample separates into three clusters that represent the end of childhood, the juvenile period, and the pubertal period. There is a separation between the sexes in all stages of development. Most notably, females begin developing earlier and complete craniofacial growth much faster than males. These results are consistent with previous studies that suggest sexual dimorphism is the product of variation in developmental trajectories between the sexes (75).

The 5–6 age-group represents the near completion of craniofacial growth and development, which marks the beginning of a slowdown in the rate of growth of the craniofacial skeleton. A slowdown in craniofacial growth continues well into the end of the juvenile period, ages 9–10, at which point the rate of growth

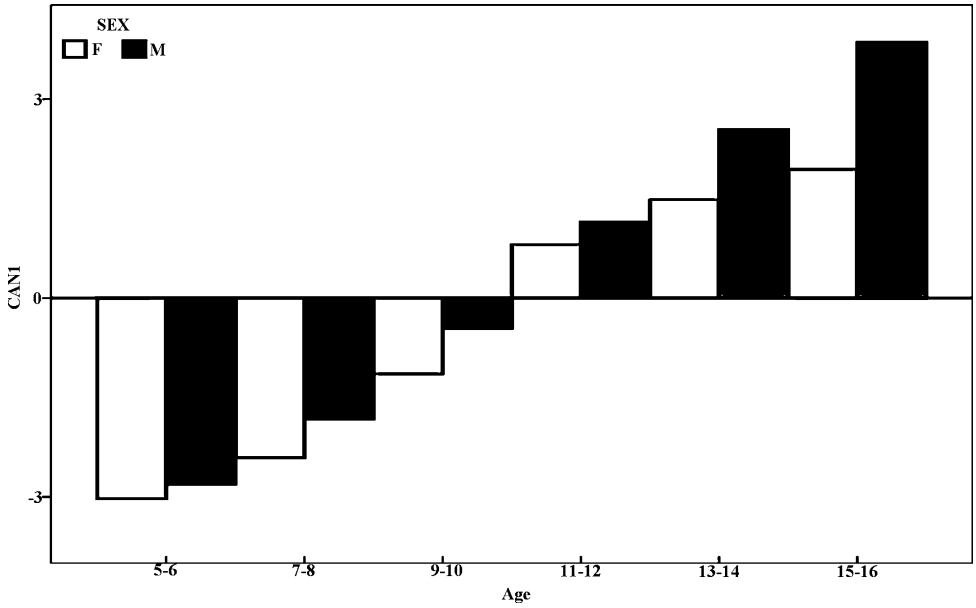

FIG. 2—*Sequence of developmental differences between the sexes in the facial skeleton. Solid bars represent males and clear bars represent females. The horizontal axis represents the age-groups in the analysis and the vertical axis represents the discriminant score means of the first canonical discriminant function for each age-group. In the vertical axis, deviations from "0" represent the degree of change in craniofacial growth. This bar graph illustrates the significance of the first canonical discriminant function in which variables influencing facial growth are most meaningful. Both sexes show a similar developmental transition from childhood to puberty. There are periods in which facial growth is slow and periods in which facial growth is faster. The 5–6 and 11–12 age-groups show the slowest facial growth changes and represent the developmental periods in which males and females are most similar. From ages 5–6 to ages 9–10 female facial growth is much faster and, consequently, females appear much lager than males. From ages 11–12 to ages 15–16 female facial growth decreases and male facial growth increases. This represents the development of secondary sexual characteristics in males.*

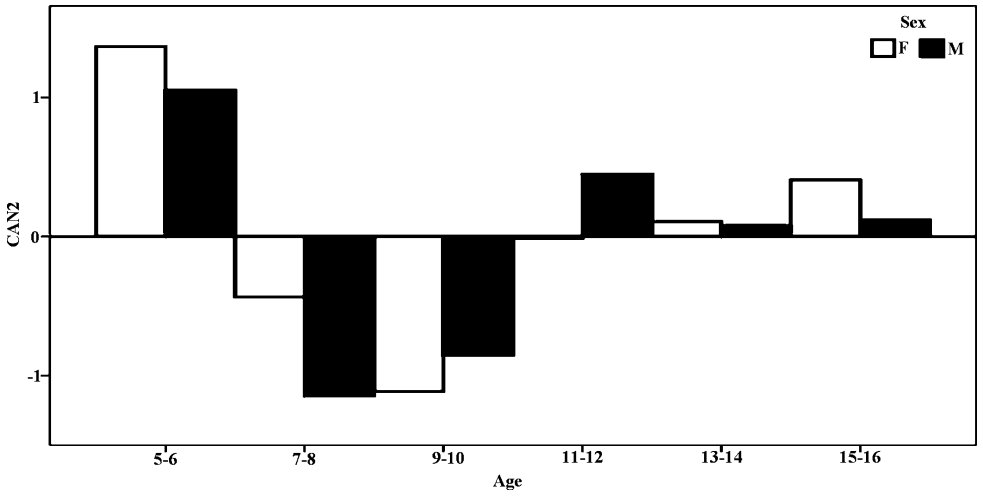

FIG. 3—*Craniofacial growth velocity differences between the sexes. Solid bars represent males and clear bars represent females. The horizontal axis represents the age-groups in the analysis and the vertical axis represents the discriminant score means of the second canonical discriminant function for each group. In the vertical axis, deviations from "0" represent the degree of change in craniofacial growth. This bar graph illustrates the significance of the second canonical discriminant function. Neurocranial and facial variables exhibit a similar pattern of change. In this function, both sexes follow a similar pattern of craniofacial growth velocity with periodic changes in the rate of craniofacial growth. This function clearly illustrates that the majority of craniofacial growth is completed around the age of six. The slight increases at the onset of puberty reflect the development of secondary sexual characteristics.*

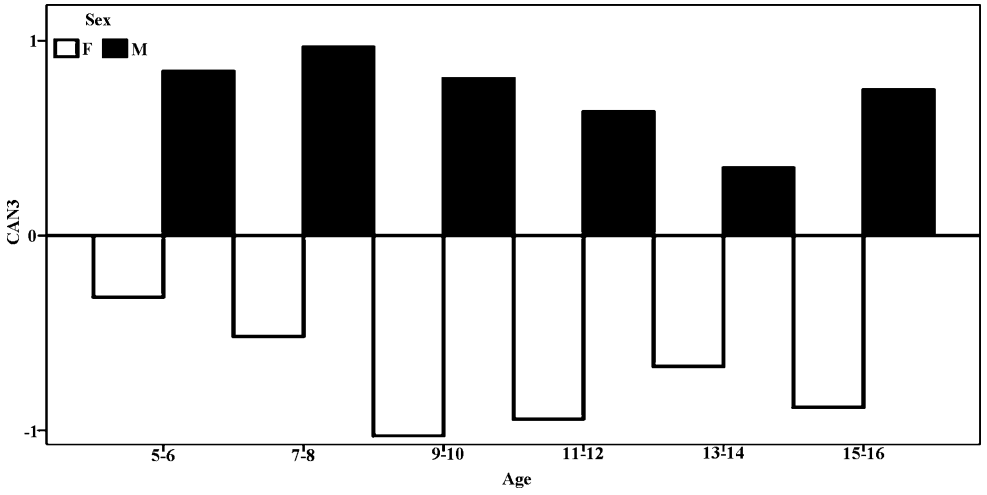

FIG. 4—*Sex differences in the juvenile craniofacial skeleton. Solid bars represent males and clear bars represent females. The horizontal axis represents the age-groups in the analysis and the vertical axis represents the discriminant score means of the third canonical discriminant function for each group. In the vertical axis, deviations from "0" represent the degree of change in craniofacial growth. This bar graph illustrates the significance of the third canonical discriminant function. Most of the variation in this function derives from neurocranial variables, which represent clear-cut difference between the sexes. This function demonstrates that sex differences in the craniofacial skeleton are established early in life. Further development of secondary sexual characteristics is the result of enhancements of already established craniofacial features that are unique to males and females.*

velocity has a slight increase that marks the beginning of puberty, the development of secondary sexual characteristics, and the culmination of craniofacial growth. The pattern shown in Fig. 5 represents changes in growth velocity that accompany important developmental events. These important developmental events represent the end of childhood, marked by the eruption of the first permanent molar, and the beginning of adolescence, marked by the eruption of the second permanent molar.

Figure 6 is a two-dimensional plot of the first and third canonical discriminant functions, which collectively account for 76.7% of the total variance. This plot illustrates facial growth changes throughout development (CAN1) and the presence of sex differences in the neurocranium (CAN3). Figure 6 shows that in all stages of development, males and females exhibit distinct morphological traits that can be observed and described. The growth interaction between all the craniofacial structures determines that pattern of sexual dimorphism.

Discriminant Functions

The most statistically meaningful variables in the canonical discriminant functions were subjected to backward stepwise discriminant analyses to create classification models for sex identification in the juvenile craniofacial skeleton. These discriminant function equations were derived from the unstandardized coefficients and the constant. The standardized coefficient indicates how much a particular variable contributes to the overall predictive value of the equation. Classification equations for sex were created for each

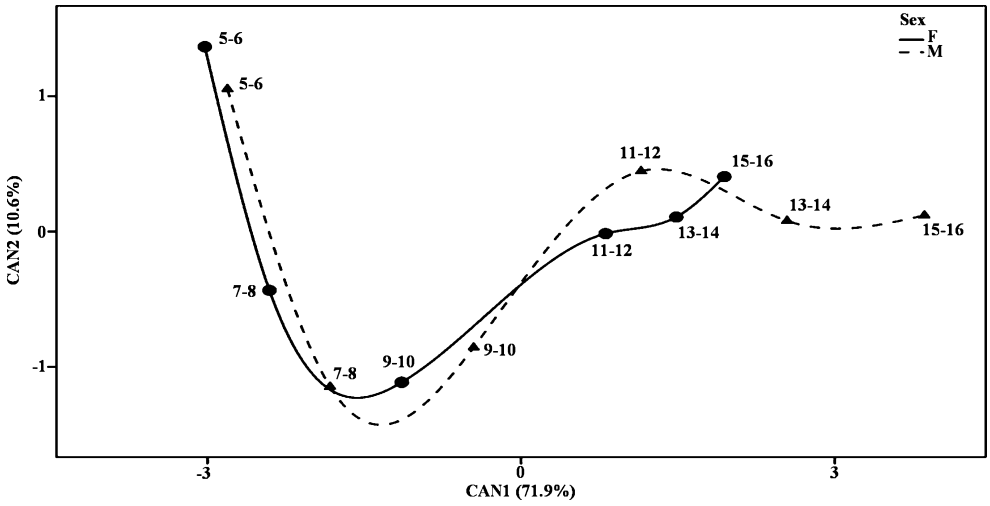

FIG. 5—*Developmental trajectories between the sexes. Females: circles with solid lines, Males: triangles with dotted lines. This two-dimensional plot represents the first and second canonical discriminant functions, which collectively account for 82.5% of the total variance. This plot illustrates a separation of the entire sample according to sex and age-group category. The data separate into three clusters: the end of childhood (ages 5–6), the juvenile period (ages 7–8 to 9–10), and the pubertal period (ages 11–12 to 15–16). Sex differentiation is evident in all developmental stages with females beginning developing earlier and completing growth much faster than males.*

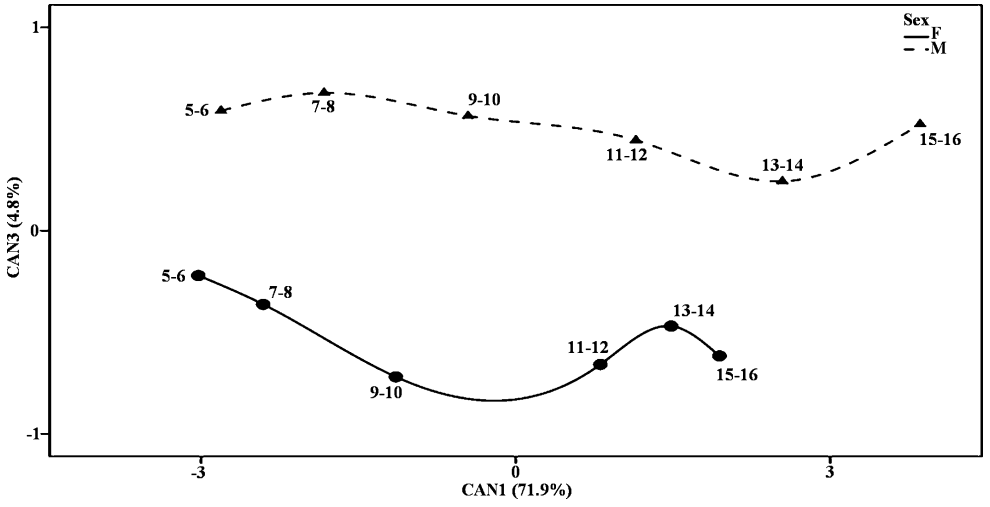

FIG. 6—*Sex differences in craniofacial growth. Females: circles with solid lines, Males: triangles with dotted lines. This two-dimensional plot represents the first and third canonical functions, which collectively account for 76.7% of the total variance. This plot shows that although sex differences are established early in the neurocranium, the expression of sexual dimorphism in the entire craniofacial complex depends on the growth interaction between all the craniofacial features.*

age-group category with sectioning points derived from the average of the group centroids for each canonical discriminant model. The most reliable model for each age-group was selected for the classification equations, which are described below (Tables 5–7).

Classification Model for Ages 5–6——Ages 5–6 (Table 5) represent the end of childhood and the beginning of the juvenile period. Craniofacial growth and development nears completion in this age-group. There is a slowdown in overall craniofacial growth as the permanent central incisors and first molars begin to erupt. The most reliable model consists of 12 variables and the constant to produce an average rate in correct classification of 78%. Correct classification dropped by 4% to an average of 74% sex identification after cross-validation. Generally, females were more correctly classified than males with opisthocranion–basion length (OBL), PNS–prosthion (PPL), and basion–nasion length (BNL) providing the greatest contribution to sex identification.

Classification Model for Ages 7–8——Ages 7–8 (Table 5) represent the eruption of the lateral incisors. It also corresponds to a further slowdown in craniofacial growth. The most reliable model consists of six variables and the constant to produce an average rate in correct classification of 80% with males having a higher rate of identification. Correct classification dropped by 2% to an average of 78% sex identification after cross-validation with males being more correctly identified than females. Basion–nasion length (BNL), bregma–opisthocranion (BOL), and nasion–bregma length (NBL) provided the greatest contribution to sex identification.

Classification Model for Ages 9–10——Ages 9–10 (Table 6) represent the eruption of the permanent canines and premolars. This age-group also corresponds to a slight increase in craniofacial growth. The most reliable model consists of 11 variables and the constant to produce an average rate in correct classification of

TABLE 5—*Discriminant functions for ages 5–8.*

Model	Variable	Unstandardized Coefficients	Standardized Coefficients	Wilks' Lambda	Canonical Correlation	Centroids	Sectioning Point	% Accuracy Original	% Accuracy Cross-Validated
Ages 5–6	PPL	1.201	2.845	0.685	0.561	F: 0.672	0	F: 80	F: 74
	NSL	−0.419	−1.057			M:−0.672		M: 76	M: 74
	OBL	0.602	3.262					Total: 78	Total: 74
	BOL	0.171	1.117						
	SPL	0.894	2.381						
	BSL	−0.373	−0.861						
	NPL	0.467	1.517						
	PNL	−0.712	−2.103						
	BBL	−0.306	−1.256						
	SOL	−0.692	−3.288						
	PSL	−1.208	−3.735						
	BNL	0.810	2.715						
	Constant	19.809							
Ages 7–8	BOL	0.142	0.950	0.609	0.625	F: −0.793	0	F: 76	F: 76
	PPL	−0.170	−0.358			M: 0.793		M: 84	M: 80
	PBL	−0.081	−0.227					Total: 80	Total: 78
	NBL	0.198	0.649						
	BNL	0.260	1.004						
	NOL	−0.141	−0.781						
	Constant	−29.547							

TABLE 6—*Discriminant functions for ages 9–12.*

Model	Variable	Unstandardized Coefficients	Standardized Coefficients	Wilks' Lambda	Canonical Correlation	Centroids	Sectioning Point	% Accuracy Original	% Accuracy Cross-Validated
Ages 9–10	PBR	0.466	2.299	0.621	0.615	F: −0.773	0	F: 86	F: 80
	PBL	0.542	1.626			M: 0.773		M: 78	M: 78
	BSL	0.542	1.246					Total: 82	Total: 79
	SPL	−0.424	−0.972						
	PNL	0.395	1.097						
	SGL	0.566	1.762						
	NPL	−0.307	−0.971						
	SOL	0.154	0.750						
	NBL	−0.286	−1.101						
	OPL	−0.184	−1.199						
	BNL	−0.772	−2.908						
	Constant	−25.176							
Ages 11–12	OBL	0.995	5.460	0.641	0.599	F: −0.740	0	F: 76	F: 70
	BSL	0.915	2.224			M: 0.740		M: 80	M: 74
	BOL	0.908	7.402					Total: 78	Total: 72
	PPL	0.650	1.663						
	PBL	0.596	2.395						
	NPL	0.370	1.169						
	BBL	−1.236	−5.639						
	SGL	1.283	3.870						
	GOL	−0.688	−4.138						
	NBL	0.922	3.883						
	PSL	−0.885	−3.592						
	NOL	−0.899	−5.134						
	Constant	−14.079							

82%. Correct classification dropped by 3% to an average of 79% sex identification after cross-validation. Generally, females were more correctly classified than males with prosthion–bregma length (PBR), sella–glabella length (SGL), and PNS–basion length (PBL) providing the greatest contribution to sex identification.

Classification Model for Ages 11–12——Ages 11–12 (Table 6) represent the eruption of the second permanent molar. The eruption of the second permanent molar signifies the beginning of the pubertal period and the onset of secondary sexual characteristics. The most reliable model consists of 12 variables and the constant to produce an average rate in correct classification of 78% with both sexes having an equal rate of identification. Correct classification dropped by 6% to an average of 72% sex identification after cross-validation. Generally, males were more correctly classified than females with bregma-opisthocranion length (BOL), opisthocranion–basion length (OBL), and nasion–bregma length (NBL) providing the greatest contribution to sex identification.

Classification Model for Ages 13–14——Ages 13–14 (Table 7) represent an inactive period in dental eruption. There are slight increases in craniofacial growth and development, which correspond to the development of secondary sexual characteristics. The most reliable model consists of 15 variables and the constant to produce an average rate in correct classification of 83%. Correct classification dropped by 5% to produce 78% sex identification after cross-validation. Generally, females were more correctly classified than males with nasion–bregma length (NBL),

TABLE 7—*Discriminant functions for ages 13–16.*

Model	Variable	Unstandardized Coefficients	Standardized Coefficients	Wilks' Lambda	Canonical Correlation	Centroids	Sectioning Point	% Accuracy Original	% Accuracy Cross-Validated
Ages 13–14	PBR	−2.344	−12.842	0.531	0.685	F: −0.931	0	F: 86	F: 80
	OBL	−0.334	−1.816			M: 0.931		M: 80	M: 76
	PPL	0.845	2.234					Total: 83	Total: 78
	SPL	0.442	1.263						
	SGL	−0.087	−0.290						
	NPL	2.070	7.363						
	PNL	−0.306	−0.900						
	BBL	0.727	3.066						
	NSL	−0.583	−1.864						
	NBL	1.835	8.326						
	GOL	0.440	2.843						
	PSL	−0.936	−3.595						
	SOL	−1.191	−6.014						
	BNL	−0.494	−1.978						
	OPL	1.056	6.686						
	Constant	−23.371							
Ages 15–16	BOL	−0.105	−0.660	0.420	0.762	F: −1.164	0	F: 88	F: 84
	BSL	0.425	1.125			M: 1.164		M: 90	M: 86
	OBL	−0.315	−1.778					Total: 89	Total: 85
	BBL	0.205	0.878						
	SGL	0.425	1.246						
	GOL	−0.448	−2.709						
	BNL	−0.323	−1.063						
	PSL	−0.226	−0.853						
	OPL	0.255	1.662						
	NOL	0.516	3.086						
	Constant	−39.242							

nasion–prosthion length (NPL), and opisthocranion–prosthion length (OPL) providing the greatest contribution to sex identification.

Classification Model for Ages 15–16——Ages 15–16 (Table 7) represent an inactive period in dental eruption. Among males, there is continued craniofacial growth, which corresponds to a further enhancement of secondary sexual characteristics. In females, there is no evidence of continued craniofacial growth, suggesting that females have ceased development. This age-group demonstrates a clear divergence between the sexes; males not finished growing while females are nearly complete. The most reliable model consists of 10 variables and the constant to produce an average rate in correct classification of 89%. Correct classification dropped by 4% to produce 85% sex identification after cross-validation. Generally, males had a higher rate of correct classification than females with nasion–opisthocranion length (NOL), opisthocranion–prosthion length (OPL), and sella–glabella length (SGL) providing the greatest contribution to sex identification.

Discussion and Conclusions

The results of this study support previous arguments that suggest sexual dimorphism in the human skeleton is the product of diverse ontogenetic origins (76). Size differences between the sexes account for most of the variation in this sample population. In both, the neurocranium and face, females have an earlier completion of growth while males complete growth much later (Fig. 2). In this study, the neurocranium is the most sexually dimorphic region of the juvenile craniofacial skeleton, until the onset of puberty. The third canonical discriminant function (Fig. 4) explains these sex differences because the most meaningful variables correspond to the neurocranium. Basion–bregma length (BBL), nasion–bregma length (NBL), sella–glabella length (SGL), bregma–opisthocranion length (BOL), and glabella–opisthocranion length (GOL) are the variables most sexually dimorphic in juveniles with males exhibiting larger dimensions than females in all stages of growth. As a result, males tend to have taller and longer heads than females. Sex differences in variables associated with the neurocranium suggests an influence of brain sexual dimorphism during growth. However, the variations in developmental growth velocity of the craniofacial skeleton shown in Fig. 3 affect the level of sexual dimorphism within each age-group. Aside from the pattern of growth velocity, the development of sexual dimorphism in the juvenile head is also influenced by factors affecting facial growth.

Unlike the growth of the neurocranium, which follows the rapid expansion of the brain, the bones of the face grow in relation to the development of the teeth, muscles of mastication, and respiratory system (26,27). Sexual dimorphism in the face becomes defined only after the onset of puberty (77). Female facial development begins to slow down around the age of 13; however, male secondary sexually dimorphic features become more distinct around the same age (77). Figure 5 demonstrates that an increase in growth velocity at the onset of puberty leads to further male morphological development in the face for several years after female growth has ceased.

The airway system is the developmental keystone for sexual dimorphism in the facial skeleton (77). Larger bodies in males require greater lung capacity to enable greater oxygen delivery to the rest of the body. Consequently, males develop a larger nasopharynx region. In contrast to females, the male nose is longer, more protrusive, and wider with a higher interorbital region, which in turn makes the supraorbital and glabellar regions more protrusive (77). Remodeling separation between the outer table and the earlier-stabilized inner table of the frontal bone gives rise to a male forehead that slopes and a female forehead that remains rounded in shape (77). In both sexes, growth of the inner table comes to an end around the ages of 5–6 when growth of the frontal lobes of the brain nears completion. The outer table, on the other hand,

continues to remodel forward until growth of the nasal region ceases (77).

Despite the independent developmental patterns of the facial and neurocranial regions, the two come together to form a functional whole. Therefore, it is critical to have an understanding of the patterns of growth described previously because sexual dimorphism in the juvenile craniofacial skeleton is ultimately derived from the growth interactions of all the craniofacial structures. For these reasons, independent analyses of the face or neurocranium will not facilitate the identification of craniofacial sexual dimorphism in juveniles.

Classification of Sex Differences in Juveniles

The growth patterns discussed previously provide the necessary insight into identifying sex differences in juvenile crania. A canonical discriminant analysis by way of a backward stepwise procedure provided the means for creating sex classification models from juvenile crania.

Each classification model provides a predictive percentage. The accuracy of sex classification follows the same trends in craniofacial developmental patterns. Prior to the onset of puberty, sex differences in the craniofacial skeleton are a reflection of brain growth. Therefore, most sexually dimorphic differences are present in the neurocranium during the juvenile period. The third canonical discriminant function represents the most meaningful variables for sex determination in the neurocranium. These variables include basion–bregma length (BBL), sella–glabella length (SGL), bregma–opisthocranion length (BOL), glabella–opisthocranion length (GOL), and nasion–opisthocranion length (NOL). Once puberty begins, facial growth takes over as the influential factor in craniofacial sexual dimorphism. The first canonical discriminant function represents the development of secondary sexual characteristics in the face. These variables include PNS–nasion length (PNL), nasion–prosthion length (NPL), prosthion–sella length (PSL), prosthion–bregma length (PBR), basion–prosthion length (BPL), basion–sella length (BSL), nasion–sella length (NSL), and opisthocranion–prosthion length (OPL).

Owing to differences in developmental timing and changes in developmental trends, neurocranial and facial measures are pooled to achieve the greatest possible classification accuracy. Therefore, a combination of neurocranial and facial variables provides the best classification models. The oldest age-group, ages 15–16, provided the best classification model for sex. Ages 7–8, 9–10, and 13–14 also provided models with high accuracy for sex. Sex identification decreased with the models derived from the 5–6 and 11–12 age-groups. Overall, sex classification in the sample ranges from 78 to 89% accuracy. It is important to keep in mind that the pattern of sex classification presented in this study corresponds to developmental trends. Fluctuations in growth over time make it difficult to isolate a specific region of the craniofacial skeleton to create classification models.

Conclusions

In conclusion, the results presented previously demonstrate the presence of sexually dimorphic differences in craniofacial growth. The pattern of craniofacial sexual dimorphism presented in this study derives from variation in the rate and timing of growth, which leads to allometric differences between the sexes. Females have a faster rate of development and cease craniofacial growth at a much earlier age than males. Sex identification depends on the recognition that the craniofacial skeleton has a modular organization. Sex expression and the ability to identify sex-specific traits vary according to age-group owing to variation in growth patterns between the neurocranium and face. Therefore, recognizing the growth variation between the sexes allows the identification of sexual dimorphism in the juvenile craniofacial skeleton.

Investigators should approach the method presented in this study with caution. If juvenile remains are recovered and the craniofacial skeleton is in good shape, radiographs of the head can be taken. If an age estimate can be derived from the dentition, then as long as the magnification factor of the X-ray machine is known, the craniometric landmarks described in this study can be identified and the radiographs measured with calipers or some other tool. The investigator will then have to convert the measurements to natural size and apply the measurements to the sex classification equations presented previously. This method is simple and practical and may be of use when genetic methods for sex identification fail to yield reliable results.

Some may argue that controlling the data for size by using techniques such as the one provided by Darroch and Mosimann (78) will eliminate the need for breaking the sample into age-groups, thus lumping all the age-groups together and creating a single discriminant function for males and females. However, the major source of variation between the sexes throughout development is size. It is through the observation of size differences that it is possible to identify important developmental events in the craniofacial skeleton and for that matter, in the rest of the skeleton. Size is an important source of variation that should not be ignored. By eliminating size from the data, the important components that contribute to sexual dimorphism, at least in this sample, will be eliminated as well. Consequently, it would not be possible to identify sex-specific variation in the data.

The results of this investigation require careful consideration and may require further study. Sample size, sample quality, sample representation, and sample treatment during an analysis can affect statistical outcomes. The data utilized in this study represent a very specific population in the United States. Therefore, the results presented here may only be representative of this population (61). The results of this study may or may not be applicable to other populations. Moreover, this study only used lateral cephalometric radiographs. As a consequence, this study does not provide a complete profile of the development of craniofacial sexual dimorphism in juveniles of European descent (61). We need to know more about craniofacial growth variation between and within populations. Fortunately, there are numerous researchers presently studying the human variation in craniofacial growth and development (79,80). Further study is necessary to make this and other juvenile identification methods acceptable to the Daubert Standard (81). Nevertheless, this investigation contributes to the growing body of work involving the study of sexual dimorphism in humans and should be viewed as the first of many studies yet to come.

Acknowledgments

I am grateful to Dr. James McNamara and the Department of Orthodontics at the University of Michigan, School of Dentistry, for allowing me access to their cephalometric radiograph collection. This research could never have been possible without their help. I am also very grateful to Dr. A.T. Steegmann, Jr. Dr. Joyce E. Sirianni, Dr. Christine Duggleby, Dr. René Bobe, and Dr. Peer H. Moore-Jansen for their continual help, support, and encouragement.

References

1. DOJ. Crime in the United States 2004. Washington, DC: Federal Bureau of Investigation, U.S. Department of Justice, 2004, http://www2.fbi.gov/ucr/cius_04/ (accessed May 15, 2009).
2. DOJ. Crime in the United States 2005. Washington, DC: Federal Bureau of Investigation, U.S. Department of Justice, 2005, http://www2.fbi.gov/ucr/05cius/ (accessed May 15, 2009).
3. DOJ. Crime in the United States 2006. Washington, DC: Federal Bureau of Investigation, U.S. Department of Justice, 2006, http://www2.fbi.gov/ucr/cius2006/index.html (accessed May 15, 2009).
4. DOJ. Crime in the United States 2007. Washington, DC: Federal Bureau of Investigation, U.S. Department of Justice, 2007, http://www2.fbi.gov/ucr/cius2007/index.html (accessed May 15, 2009).
5. Pretorius E, Steyn M, Scholtz Y. Investigation into the usability of geometric morphometric analysis in assessment of sexual dimorphism. Am J Phys Anthropol 2006;129:64–70.
6. Rogers TL. Determining the sex of human remains through cranial morphology. J Forensic Sci 2005;50:493–500.
7. Bailit H, Hunt E. The sexing of children's skeletons from teeth alone and its genetic implications. Am J Phys Anthropol 1964;22:171–4.
8. Black TK. Sexual dimorphism in the tooth crown diameters of the deciduous teeth. Am J Phys Anthropol 1978;48:77–82.
9. Boucher BJ. Sex differences in the foetal sciatic notch. J Forensic Med 1955;2:51–4.
10. Boucher BJ. Sex differences in the foetal pelvis. Am J Phys Anthropol 1957;15:581–600.
11. Coleman WH. Sex differences in the growth of the human bony pelvis. Am J Phys Anthropol 1969;31:125–52.
12. DeVito C, Saunders SR. A discriminant function analysis of deciduous teeth to determine sex. J Forensic Sci 1990;35:845–58.
13. Ditch LE, Rose JC. A multivariate dental sexing technique. Am J Phys Anthropol 1972;37:61–4.
14. Fazekas I, Kósa F. Forensic fetal osteology. Budapest, Hungary: Akadémiai Kiadó, 1978.
15. Garn SM, Cole P, Van Alstine W. Sex discriminatory effectiveness using combinations of root lengths and crown diameters. Am J Phys Anthropol 1979;50:115–8.
16. Hunt DR. Sex determination in the subadult ilia: an indirect test of weaver's non-metric sexing method. J Forensic Sci 1990;35:881–5.
17. Hunt E, Gleiser I. The estimation of age and sex of preadolescent children from bones and teeth. Am J Phys Anthropol 1955;13:479–87.
18. Mittler D, Sheridan S. Sex determination in subadults using auricular surface morphology: a forensic science perspective. J Forensic Sci 1992;37:1068–75.
19. Molleson TI, Cruse K, Mays S. Some sexually dimorphic features of the human juvenile skull and their value in sex determination in immature skeletal remains. J Archaeol Sci 1998;25:719–28.
20. Rösing FW. Sexing immature skeletons. J Hum Evol 1983;12:149–55.
21. Schutkowski H. Sex determination of infant and juvenile skeletons I: morphognostic features. Am J Phys Anthropol 1993;90:199–205.
22. Schutkowski H. Sex determination of fetal and neonatal skeletons by means of discriminant analysis. Int J Anthropol 1987;2:347–52.
23. Ursi W, Trotman C, McNamara J Jr, Behrents R. Sexual dimorphism in normal craniofacial growth. Angle Orthod 1993;63(1):47–56.
24. Weaver D. Sex differences in the ilia of a known sex and age sample of fetal and infant skeletons. Am J Phys Anthropol 1980;52:191–5.
25. Komar DA, Buikstra JE. Forensic anthropology: contemporary theory and practice. Oxford, UK: Oxford University Press, 2008.
26. Scheuer L, Black S. The juvenile skeleton. New York, NY: Academic Press, 2004.
27. Scheuer L, Black S. Developmental juvenile osteology. New York, NY: Academic Press, 2000.
28. Hagelberg E, Clegg J. Isolation and characterization of DNA from archaeological bones. Proc R Soc Lond 1991;244:45–50.
29. Hagelberg E, Sykes B, Hedges R. Ancient bone DNA amplified. Nature 1989;342:485.
30. Naito E, Dewa K, Yamanouchi H, Kominami R. Sex typing of forensic DNA samples using male and female specific probes. J Forensic Sci 1994;39(4):1009–17.
31. Akane A. Sex determination by PCR analysis of the X-Y amelogenin gene. Methods Mol Biol 1998;98:245–9.
32. Lau E, Mohandas T, Shapiro L, Slavkin H, Snead M. Human amelogenin gene loci are on the X and Y chromosomes. Am J Hum Genet 1988;43:A149.
33. Roccazzello A, Tringali G, Barbaro A, Cormaci P, Barbaro A, Insirello E. Simultaneous estimation of a Y-specific fragment, and X-specific fragment, and sex determination of forensic studies in real-time PCR. Forensic Sci Int 2004;146S:165–6.
34. Stone A, Päbo S, Stoneking M. Sex determination of ancient human skeletons using DNA. Am J Phys Anthropol 1996;99:231–8.
35. Alonso A, Martín P, Albarrán C, García P, García O, Fernández de Simón L, et al. Real time PCR designs to estimate nuclear and mitochondrial DNA copy number in forensic and ancient DNA studies. Forensic Sci Int 2004;139:141–9.
36. Andréasson H, Allen M. Rapid quantification and sex determination of forensic evidence materials. J Forensic Sci 2003;48:1–8.
37. Gotherstrom A, Liden K, Ahlstrom T, Kallersjo M, Brown TA. Osteology, DNA, and sex identification: morphological and molecular sex identification of five Neolithic individuals from Ajvide, Gotland. Int J Osteoarchaeol 1997;7:71–81.
38. Mays S, Faerman M. Sex identification in some putative infanticide victims from Roman Britain using ancient DNA. J Archaeol Sci 2001;28:555–9.
39. Yamamoto T, Uchihi R, Kojima T, Nozawa H, Huang X, Tamaki K, et al. Maternal identification from skeletal remains of an infant kept by alleged mother 16 years with DNA typing. J Forensic Sci 1998;43:701–5.
40. Brown K. Ancient DNA and archaeology-practical advice for field practice. SAS Bulletin 2003;26:3–4.
41. Cooper A, Poiner H. Ancient DNA: do it right or not at all. Science 2000;289:1139.
42. Hofreiter M, Serre D, Poinar H, Kuch M, Päbo S. Ancient DNA. Nat Genet 2001;2:353–9.
43. Richards M. Sampling procedure for bone chemistry. In: Brickley M, McKinley J, editors. Guidelines to the standards for recording human remains. Southampton, UK: British Association for Biological Anthropology and Osteoarchaeology, Institute of Field Archaeologists, 2004;Paper No. 7;43–5.
44. Ye J, Ji A, Parra E, Zheng X, Jiang C, Zhao X, et al. A simple and efficient method for extracting DNA from old and burned bone. J Forensic Sci 2004;49:1–6.
45. Yao Y, Bravi C, Bandelt H. A call for mtDNA data quality control in forensic science. Forensic Sci Int 2004;141:1–6.
46. Arismendi J, Baker L, Matteson K. Effects of processing techniques on the forensic DNA analysis of human skeletal remains. J Forensic Sci 2004;49:930–4.
47. Lindahl T. Instability and decay on the primary structure of DNA. Nature 1993;362:709–15.
48. Tuross N. The biochemistry of ancient DNA in bone. Experientia 1994;50:530–5.
49. Gilbert TP, Willerslev E, Hansen AJ, Barnes I, Rudbeck L, Lynnerup N, et al. Distribution patterns of postmortem damage in human mitochondrial DNA. Am J Hum Genet 2003;72:32–47.
50. Gilbert TP, Hansen AJ, Willerslev E, Rudbeck L, Barnes I, Lynnerup N, et al. Characterization of genetic miscoding lesions caused by postmortem damage. Am J Hum Genet 2003;72:48–61.
51. Ackermann R, Krovitz G. Common patterns of facial ontogeny in the hominid lineage. Anat Rec 2002;269:142–7.
52. Guihard-Costa A, Ramirez-Rozzi F. Growth of the human brain and skull slows down at about 2.5 years old. C R Palevol 2004;3:397–402.
53. Smith B. Dental development and the evolution of life history in hominidae. Am J Phys Anthropol 1991;86:157–74.
54. Ceballos J, Rentschler E. Roentgen diagnosis of sex based on adult skull characteristics. Comparison study of cephalometry of male and female skull films (frontal projection). Radiology 1958;70:55–61.
55. Townsend GC, Richards LC, Carroll A. Sex determination of Australian aboriginal skulls by discriminant function analysis. Aust Dent J 1982;27:320–6.
56. Hsiao T, Chang H, Liu K. Sex determination by discriminant function analysis of lateral radiographic cephalometry. J Forensic Sci 1996;41:792–5.
57. Patil K, Mody R. Determination of sex by discriminant function analysis and stature by regression analysis: a lateral cephalometric study. Forensic Sci Int 2005;147:175–80.
58. Veyre-Goulet S, Mercier C, Robin O, Guérin C. Recent human sexual dimorphism study using cephalometric plots on lateral teleradiography and discriminant function analysis. J Forensic Sci 2008;53(4):786–9.
59. Bulygina E, Mitteroecker P, Aiello L. Ontogeny of facial dimorphism and patterns of individual development within one human population. Am J Phys Anthropol 2006;131(3):432–43.

60. Riolo M, McNamara J, Hunter W. An atlas of craniofacial growth. Ann Arbor, MI: The University of Michigan, Center for Human Growth and Development, 1974.
61. Gonzalez RA. Sexual dimorphism in the craniofacial form of North American juveniles of European descent [dissertation]. Buffalo (NY): State University of New York at Buffalo, 2006.
62. Dibbets J. Applicability of cephalometric standards: an appraisal of atlases. In: Trotman C, McNamara J, editors. Orthodontic treatment: outcome and effectiveness. Ann Arbor, MI: Center for Human Growth and Development, The University of Michigan, 1995;297–317.
63. Leigh S. Evolution of human growth spurts. Am J Phys Anthropol 1996;101:455–74.
64. Bass WM. Human osteology: a laboratory and field manual, 5th edn. Columbia, MO: Missouri Archaeological Society, 2005.
65. Enlow DH, Poston WR. Facial growth. Philadelphia, PA: W.B. Saunders Company, 1990.
66. Howells WW. Cranial variation in man. Cambridge, UK: Peabody Museum of Archeology and Ethnology, Harvard University, 1973.
67. SPSS Inc. SPSS base 9.0 applications guide. Chicago, IL: SPSS Inc. 1999.
68. Dibbets J, Nolte K. Comparison of linear cephalometric dimensions in Americans of European descent (Ann Arbor, Cleveland, Philadelphia) and Americans of African descent (Nashville). Angle Orthod 2002;72:324–30.
69. Lestrel PE. Morphometrics of craniofacial form. In: Dixon AD, Hoyte D, Rönning O, editors. Fundamentals of craniofacial growth. New York, NY: CRC Press, 1997;155–87.
70. Klecka WR. Discriminant analysis. London, UK: Sage Publications, 1980.
71. Duarte Silva AP, Stam A. Discriminant analysis. In: Grimm L, Yarnold P, editors. Reading and understanding multivariate statistics. Washington, DC: American Psychological Association, 1995;277–318.
72. Campbell N. Multivariate analysis in biological anthropology: some further considerations. J Hum Evol 1978;7:197–203.
73. Pietrusewsky M. Metric analysis of skeletal remains: methods and applications. In: Katzenberg M, Saunders SR, editors. Biological anthropology of the human skeleton. New York, NY: Wiley-Liss, 2000;375–415.
74. Manly B. Multivariate statistical methods: a primer. London, UK: Chapman and Hall, 1986.
75. Shea BT. Ontogenetic approaches to sexual dimorphism in anthropoids. J Hum Evol 1986;1:97–110.
76. Humphrey L. Growth patterns in the modern human skeleton. Am J Phys Anthropol 1998;105:57–72.
77. Enlow D, Hans M. Essentials of facial growth. Philadelphia, PA: W.B. Saunders Company, 1996.
78. Darroch J, Mosimann J. Canonical and principal components of shape. Biometrka 1985;72:241–52.
79. Buck TJ, Vidarsdóttir US. A proposed method for the identification of race in sub-adult skeletons: a geometric morphometric analysis of mandibular morphology. J Forensic Sci 2004;49(6):1159–64.
80. Vidarsdóttir US, O'Higgins P, Stringer C. A geometric morphometric study of regional differences in the ontogeny of the modern human facial skeleton. J Anat 2002;201:211–29.
81. *Daubert v. Merrell Dow Pharmaceuticals, Inc.,* 509 U.S. 579, 1993.

Additional information and reprint requests:
Richard A. Gonzalez, Ph.D.
Department of Physical Therapy
Clarkson University
Clarkson Hall
59 Main St.
Potsdam, NY 13699
E-mail: rgonzale@clarkson.edu